Clinical Pharmacokinetics (2021) 60:1621–1633
https://doi.org/10.1007/s40262-021-01039-5

ORIGINAL RESEARCH ARTICLE

Population Cellular Kinetics of Lisocabtagene Maraleucel, an Autologous CD19-Directed Chimeric Antigen Receptor T-Cell Product, in Patients with Relapsed/Refractory Large B-Cell Lymphoma

Ken Ogasawara[1] · Michael Dodds[2] · Timothy Mack[1] · James Lymp[3] · Justine Dell'Aringa[3] · Jeff Smith[3]

Accepted: 11 May 2021 / Published online: 14 June 2021

Abstract

Background and Objectives Lisocabtagene maraleucel (liso-cel) is a CD19-directed, defined composition, 4-1BB chimeric antigen receptor (CAR) T-cell product administered at equal target doses of $CD8^+$ and $CD4^+$ CAR^+ T cells. Large between-subject variability has been noted with CAR T-cell therapies; patient characteristics might contribute to CAR T-cell expansion variability. We developed a population cellular kinetic model to characterize the kinetics of the liso-cel transgene, via quantitative polymerase chain reaction assessment after intravenous infusion of liso-cel, and to understand covariates that might influence liso-cel kinetics in individual patients.

Methods We employed nonlinear mixed-effects modeling to develop a population cellular kinetic model for liso-cel. The population cellular kinetic analysis was performed using 2524 post-infusion transgene observations from 261 patients with relapsed/refractory large B-cell lymphoma who were treated with a single dose of liso-cel in TRANSCEND NHL 001. Covariates for the analysis included baseline intrinsic factors such as age, baseline disease characteristics, and liso-cel and coadministration factors.

Results Liso-cel cellular kinetics were well described by a piecewise model of cellular growth kinetics that featured lag, exponential growth, and biexponential decay phases. Population means (95% confidence interval) of lag phase duration, doubling time, time to maximum levels, initial decline half-life, and terminal half-life were 3.27 (2.71–3.97), 0.755 (0.667–0.821), 9.29 (8.81–9.70), 5.00 (4.15–5.90), and 352 (241–647) days, respectively. The magnitude of effect on liso-cel expansion metrics demonstrated that the covariate associations were smaller than the residual between-subject variability in the population.

Conclusions The covariates tested were not considered to have a meaningful impact on liso-cel kinetics.

Clinical Trial Registration NCT02631044.

1 Introduction

Lisocabtagene maraleucel (liso-cel; JCAR017) is a CD19-directed, genetically modified, defined composition, autologous cellular immunotherapy administered at equal target doses of $CD8^+$ and $CD4^+$ chimeric antigen receptor (CAR)-positive T cells [1]. The CAR comprises an FMC63 monoclonal antibody-derived single-chain

Key Points

A population cellular kinetic model of lisocabtagene maraleucel (liso-cel), a CD19-directed chimeric antigen receptor T-cell product, was developed to characterize the kinetics of the liso-cel transgene in relapsed/refractory large B-cell lymphoma.

Liso-cel cellular kinetics were well described by a piecewise model of cellular growth kinetics that featured lag, growth, and biphasic decay phases.

The covariates tested were not considered to have a meaningful impact on liso-cel kinetics.

Previous Presentation: None.

✉ Ken Ogasawara
ken.ogasawara@bms.com

[1] Bristol Myers Squibb, Princeton, NJ, USA

[2] Certara, Princeton, NJ, USA

[3] Bristol Myers Squibb, Seattle, WA, USA

variable fragment, immunoglobulin G4 hinge region, CD28 transmembrane domain, 4-1BB (CD137) costimulatory domain, and CD3ζ activation domain [2]. In addition, liso-cel includes a nonfunctional truncated epidermal growth factor receptor that is coexpressed on the cell surface with the CD19-specific CAR and can serve as a surrogate for CAR expression [3–5]. CAR binding to CD19 expressed on the cell surface of tumors and normal B cells induces activation and proliferation of CAR T cells, release of proinflammatory cytokines, and cytotoxic killing of target cells [6].

TRANSCEND NHL 001 (TRANSCEND; NCT02631044) is a multicenter, multicohort, open-label, seamless design (i.e. consisting of dose-finding, dose-expansion, and dose-confirmation phases) study to determine the safety, antitumor activity, and cellular kinetics of liso-cel in patients with relapsed/refractory large B-cell lymphoma (LBCL; LBCL cohort) and mantle cell lymphoma (mantle cell lymphoma cohort). TRANSCEND is the largest clinical study reported to date of CD19-directed CAR T-cell therapy in relapsed/refractory LBCL [1, 3, 7–9]. Eligible patients underwent leukapheresis for collection of autologous peripheral blood mononuclear cells for manufacture of liso-cel followed by lymphodepleting chemotherapy (LDC; fludarabine 30 mg/m^2 and cyclophosphamide 300 mg/m^2 for 3 days) [1]. During the liso-cel manufacturing process (between leukapheresis and LDC), bridging therapy with systemic and/or radiation therapy was allowed at the discretion of the treating physician. Liso-cel was administered as two sequential infusions of CD8$^+$ and CD4$^+$ CAR$^+$ T cells at one of three dose levels (50×10^6, 100×10^6, or 150×10^6 CAR$^+$ T cells). The 269 patients who received liso-cel had a median age of 63 years and a median of three previous lines of systemic therapy; 67% had chemotherapy-refractory disease, 33% had previous autologous hematopoietic stem cell transplantation (HSCT), and 59% received bridging therapy. In efficacy-evaluable patients ($n = 256$), treatment with liso-cel resulted in a high rate of durable complete response (CR), with an objective response rate of 73%, CR rate of 53%, and an estimated duration of CR at 1 year of 65% [1]. Liso-cel treatment was associated with a low incidence of severe cytokine release syndrome (CRS; 2%) and neurological events (NEs; 10%). CRS of any grade was reported in 42% of patients, with median time to onset of 5 days and median time to resolution of 5 days. NEs of any grade were reported in 30% of patients, with median time to onset of 9 days and median time to resolution of 11 days. Additional safety outcomes of interest included severe neutropenia (60%), anemia (37%), and thrombocytopenia (27%), with prolonged cytopenia (not resolved at Day 29) in 37% of patients. Severe infections, including bacterial, fungal, and viral, were reported in 12% of patients.

Cellular kinetics of two other CAR T-cell therapies (tisagenlecleucel and axicabtagene ciloleucel [axi-cel]) were characterized in B-cell acute lymphoblastic leukemia (B-ALL; tisagenlecleucel) [10–12] and relapsed/refractory LBCL (tisagenlecleucel [13] and axi-cel [8]). These CAR T-cell therapies generally showed rapid in vivo expansion within 2 weeks post-infusion followed by subsequent biexponential decline [8, 12]. In TRANSCEND, median time to liso-cel peak expansion was 12 days, and higher liso-cel expansion was associated with higher rates of CR and partial response (maximum transgene levels [C_{max}], 3.55-fold) and higher incidence of CRS (C_{max}, 2.29-fold) and NEs (C_{max}, 3.34-fold) in patients with relapsed/refractory LBCL [1]. Liso-cel was present in peripheral blood for up to 2 years [1]. Large between-subject variability (BSV) was noted in all three CAR T-cell therapies (e.g. percentage coefficient of variation [%CV] of > 100% for tisagenlecleucel) [12, 13], as expected for biologic products that expand in vivo; patient characteristics might also contribute to the variability of CAR T-cell expansion. Tisagenlecleucel expansion was lower in LBCL than B-ALL [13]. Patient demographics such as age and sex had no significant impact on the expansion of both tisagenlecleucel and axi-cel [14, 15]; however, these findings might be because of the relatively small sample size given the large BSV. TRANSCEND is the largest clinical study among CD19-directed CAR T-cell therapies, and in this study the association of baseline intrinsic and disease factors with liso-cel kinetics was investigated. This study describes a population cellular kinetic model of liso-cel that was developed to characterize the kinetics of the liso-cel transgene in relapsed/refractory LBCL, as assessed by quantitative polymerase chain reaction (qPCR) after intravenous infusion of liso-cel, and to understand covariates that might influence liso-cel kinetics in individual patients.

2 Methods

2.1 Clinical Study Data

The population cellular kinetic analysis was performed using data from the LBCL cohort of TRANSCEND for three dose levels (50×10^6, 100×10^6, or 150×10^6 CAR$^+$ T cells) on a single-dose schedule [1]. Based on dose-limiting toxicities and activity observed during the dose-finding and dose-expansion phases, dose level 2 (100×10^6 CAR$^+$ T cells) was selected for evaluation during the dose-confirmation phase. For patients who were on a single-dose schedule and received re-treatment with or additional cycles of liso-cel, data after re-treatment or additional cycles (maximum, two cycles) were excluded from the analysis. Follow-up for the TRANSCEND LBCL cohort was ongoing as of 12 August 2019, the data cut-off date used for this analysis. The study

was conducted in accordance with the Declaration of Helsinki, International Conference on Harmonisation Good Clinical Practice guidelines, and applicable regulatory requirements. Institutional Review Boards approved the study protocol and amendments at participating institutions. All patients provided written informed consent.

2.2 Bioanalytical Methods

Blood samples for determination of the liso-cel transgene were collected at pre-infusion and 1, 3, 7, 10, 14, 21, and 28 days and 2, 3, 6, 9, 12, 18, and 24 months post-infusion. Liso-cel transgene levels in peripheral blood were measured using a validated real-time qPCR assay, which is an accepted approach for evaluating cellular kinetics of CAR T-cell therapies. Liso-cel vector copy number was determined through the quantification of two genes: (1) woodchuck hepatitis virus post-transcriptional regulatory element (WPRE), a post-transcriptional regulatory element present in the lentiviral vector used to transduce the gene that encodes for liso-cel into cells; and (2) human albumin, a housekeeping gene used to normalize genomic DNA for each sample. DNA was extracted from cells after the removal of plasma using QIAamp DNA Isolation Kits, quantified, and stored until analysis. Samples were analyzed in a duplex reaction at a DNA input of 200 ng per reaction using a proprietary assay that quantifies WPRE and albumin. Results were reported as WPRE copies/µg of DNA, which was determined based on the number of WPRE copies normalized to the number of albumin copies/reaction (assuming 2 albumin copies/genome and 6.6 pg DNA/genome). The limit of detection of WPRE was determined to be 5 copies/reaction. Inter- and intra-assay precision was evaluated using prepared quality control samples. The inter-assay precision (%CV) was $\leq$ 30% for albumin and $\leq$ 25% for WPRE, while the intra-assay precision for WPRE and albumin was $\leq$ 20% for all levels, except at the lower limit of quantification where it ranged from 3% to 57%.

2.3 Population Cellular Kinetic Modeling Analysis

Overall, 2524 post-infusion transgene observations from 261 patients were used in the population cellular kinetic analyses. Of these, 394 (16%) were below the limit of detection and were flagged as missing. This primarily occurred in the extreme end of post-treatment follow-up. Population cellular kinetic models were developed using a nonlinear mixed-effect modeling approach, as implemented in NONMEM version 7.3.0 (ICON Development Solutions, Ellicott City, MD, USA) and Perl-speaks-NONMEM [16]. Data management and graphical evaluations were performed in R version 3.3.2 (The R Foundation, Vienna, Austria).

First, the first-order conditional estimation with eta-epsilon interaction (FOCEI) method was used to approximate the objective function value (OFV). The FOCEI OFV is a linear approximation of the true OFV. Next, the final parameter values from the FOCEI step were used as starting values for the importance sampling method to further refine the solution and response surface without OFV approximation [17]. The variance–covariance matrix was derived from the importance sampling step, and parameter relative standard error estimates were produced without OFV linearization. Finally, 500 replicate bootstrap data sets were generated using sampling without replacement to produce the 2.5th and 97.5th percentiles of the parameters.

2.4 Structural Model

Systemic disposition of CAR T-cell therapies such as liso-cel have been previously described by a piecewise model embodying an initial cellular expansion phase followed by a biphasic contraction phase based on theoretic work by De Boer and Perelson [10, 18, 19]. The specific form was taken from the case where vigorous immune responses are evoked (e.g. in the presence of a rapidly replicating pathogen). Under these circumstances, T-cell proliferation is triggered rapidly and not limited by antigens, leading to all T cells proliferating at their maximal rate for some period. After this time, all T cells enter a contraction phase, where activated T cells either rapidly die out or transition to longer-lived memory T cells. This structural model was used as the starting model and was refined as necessary to adequately describe the data among patients. The model was fit to logarithmically transformed liso-cel transgene levels. Adequacy of the model to describe the data was evaluated using standard goodness-of-fit criteria, including observations versus population and individual predictions and conditional weighted residuals (CWRES) versus population predictions and time.

The exponential model was used for the description of BSV in cellular kinetic parameters. BSV on model parameters was introduced in terms of random between-subject effects as follows (Eq. 1):

$$\theta_{k,i} = \theta_k \times e^{\eta_{k,i}} \quad (1)$$

where θ_k denotes the typical population parameter estimate for the *kth* parameter, $\theta_{k,i}$ denotes the parameter estimate for the *kth* parameter in the *ith* subject, and $\eta_{k,i}$ denotes the between-subject random effect for the *ith* subject, where $\eta_{k,i}$ is assumed to have a mean of 0 and an estimated variance of ω^2. BSV on a model parameter was retained if supported by the data (i.e. if estimates did not cause model instability and shrinkage was < 30%) [20]. A logit-transformed parameter was used to introduce BSV in the case of parameters with domain [0,1] (i.e. when describing the fraction of activated T cells that transition to memory T cells). However,

BSV for this parameter was dropped because of poor estimate quality for this BSV term. The inclusion of off-diagonal elements was investigated but was not supported based on pairwise plots of individual η estimates. Additive error models were used to describe residual variability after the model predictions were logarithmically transformed. The statistical model was assessed with the diagnostic plots, including histograms of η estimates and pairwise plots of individual η estimates.

2.5 Covariate Model

Covariate modeling focused on identifying and quantifying covariates that explain BSV in cellular kinetic parameters among patients. Covariates for the analysis included:

- Baseline intrinsic factors: age, body size (by body weight and body mass index), sex, race, ethnicity, creatinine clearance by Cockcroft–Gault equation, alanine aminotransferase, aspartate aminotransferase, and left ventricular ejection fraction (≥ 40% to < 50% or ≥ 50%).
- Baseline disease factors: lactate dehydrogenase (LDH) before LDC, sum of the product of perpendicular diameters (SPD) per Independent Review Committee (IRC) before LDC, C-reactive protein, LBCL subtype, secondary central nervous system lymphoma, Eastern Cooperative Oncology Group performance status at screening, prior lines of systemic therapy, prior response status, prior chemotherapy response status, and prior HSCT.
- Liso-cel and coadministration factors: administered dose of liso-cel, bridging therapy after leukapheresis, and tocilizumab and/or corticosteroid use for CRS or NE treatment.

Covariate inclusion in the model was guided by the following considerations: graphical exploration against random effects in the model, clinical and physiological considerations, and results of the prespecified covariate search applied to noncompartmental analysis results. Missing covariates were imputed as the median value in the study population.

A forward-addition and backwards-elimination stepwise covariate modeling approach was used to add covariates to the model based on these considerations. The likelihood ratio test was used to evaluate the statistical significance of incorporating or removing each respective covariate in the model. For forward addition and backward elimination, significance levels (α) of 0.01 and 0.001, respectively, were employed.

Continuous covariates were centered on a typical value (e.g. median of the study population). Relationships between cellular kinetic parameters and continuous covariates were described as a linear model as follows (Eq. 2):

$$P_{k,i} = P_k \times \left[1 + \theta \bullet \left(cov_i - med_{cov}\right)\right] \quad (2)$$

where $P_{k,i}$ is the individual value of the cellular kinetic parameter k, P_k is the typical value of the cellular kinetic parameter k, cov_i is the individual covariate value, med_{cov} is the median covariate value of the study population, and θ is the scaling parameter for the range of the covariate. All covariates (except age) were log-transformed; thus, this linear model formulation was equivalent to a power model formulation for these covariates.

Binary categorical covariates were incorporated into the model as index variables described as follows (Eq. 3):

$$P_{k,i} = P_k \times (1 + \theta^{cov_i}) \quad (3)$$

where cov_i is the individual covariate value for a binary covariate with possible values of 0 and 1. Categorical covariates with multiple values were implemented as products of the binary covariate model.

2.6 Model Evaluation

A final NONMEM model was expected to meet the following criteria: (1) a 'minimization successful' statement by the NONMEM program; (2) three or more significant digits for all parameters; (3) parameter estimates that were judged to be clinically meaningful and not close to a boundary; and (4) good agreement between observations and predictions in standard goodness-of-fit plots. Bootstrap resampling techniques were used to evaluate the stability of the final model and to estimate confidence intervals (CIs) for the model parameters. The predictive performance of the model was assessed by a visual predictive check. Observed data and 500 replicate simulations from the final model were summarized by median and 5th/95th percentiles, respectively.

2.7 Simulations

The final population cellular kinetic model was used to simulate individual liso-cel cellular kinetic parameters: C_{max}, time to maximum transgene levels (T_{max}), and area under the curve for transgene levels from 0 to 28 days post-infusion ($AUC_{0–28d}$). Covariate values in the model were given by observed values in TRANSCEND, thus preserving any collinearity between covariates. Random effects were sampled from the estimated variance–covariance matrices 300 times for each of the 261 patients, yielding 78,300 simulated patients. Fixed effects were given from the population estimates. Forest plots were used to explore the impact of significant covariates on liso-cel expansion metrics. Stochastic simulations using the final population cellular kinetic model were performed to show the expected impact on liso-cel expansion in subpopulations of interest.

3 Results

3.1 Patients

The population cellular kinetic data set included data from 261 patients in TRANSCEND. Table 1 shows the patients' demographic and clinical characteristics that were included as covariates of the patient data set. Median age was 63 years (range 18–86). Twenty-eight percent of patients received either tocilizumab or corticosteroids, or both, for the treatment of CRS and/or NEs.

3.2 Structural Population Cellular Kinetic Model of Liso-cel

A piecewise model embodying an initial cellular expansion phase, followed by a biphasic contraction phase, was fit to the liso-cel transgene data. Notable discrepancies in the first 3 days post-infusion were observed. Specifically, the model-predicted expansion phase overpredicted early time points and transgene levels near their peak values. The model was expanded to include four classical phases of cellular growth: lag, growth, stationary, and decay [21]. Adding a lag phase to the initial cellular expansion phase improved model fit. The addition of a stationary phase did not improve model fit and was discarded.

Figure 1 shows the final form of the structural model for liso-cel transgene levels. After infusion (t = 0), liso-cel transgene levels were stationary during the lag phase. The duration of the lag phase was defined as T_{lag}, during which time liso-cel levels were constant initial transgene levels (C_0). During the lag phase, liso-cel transgene levels were given as (Eq. 4):

$$C(t) = C_0 = C_{max}/2^{\frac{T_{gro}}{T_{dbl}}} \text{ when } 0 \le t < T_{lag} \quad (4)$$

which is a simple rearrangement of the C(t) expression below, substituting $t = T_{max} = T_{lag} + T_{gro}$ and $C(t) = C_{max}$. After the lag phase ($t = T_{lag}$), liso-cel transgene levels doubled every interval (T_{dbl}) during the growth phase, reflecting doubling of infused T cells bearing liso-cel transgene by mitotic cell division. The duration of the growth phase was defined as T_{gro}, at which time ($T_{max} = T_{lag} + T_{gro}$) liso-cel transgene levels reached C_{max}. During the growth phase, liso-cel transgene levels were given as (Eq. 5):

$$C(t) = C_0 \bullet 2^{\frac{(t-T_{lag})}{T_{dbl}}} \text{ when } T_{lag} \le t < T_{lag} + T_{gro} \quad (5)$$

After the growth phase ($t = T_{max} = T_{lag} + T_{gro}$), liso-cel transgene levels declined in a biphasic manner during the decay phase. A fraction of liso-cel transgene signal at C_{max} that appears in the β or terminal phase with half-life HL_β was F_β. One minus that fraction appeared in the α phase with half-life HL_α. During the decay phase, liso-cel transgene levels were given as (Eq. 6):

$$C(t) = C_{max} \bullet \left((1 - F_\beta) \bullet 2^{\frac{-(t-T_{max})}{HL_\alpha}} + F_\beta \bullet 2^{\frac{-(t-T_{max})}{HL_\beta}} \right) \text{ when } T_{lag} + T_{gro} \le t < \infty \quad (6)$$

Random effects for T_{gro}, F_β, and HL_β were removed from the model because the η shrinkage exceeded 30%. The remaining random effects were centered around 0, normally distributed, and showed little correlation, except for the random effects for C_{max} and T_{dbl} that had a correlation coefficient of $r = -0.459$. This would suggest that patients with high C_{max} (maximal liso-cel transgene levels after expansion) have a short T_{dbl} (doubling time of liso-cel transgene levels during expansion). However, the correlation coefficient dropped to $r = -0.352$ after additions of all covariates in the final model, suggesting a weak correlation after covariate addition. Thus, a diagonal variance–covariance matrix structure was selected.

3.3 Final Population Cellular Kinetic Model of Liso-cel

Population cellular kinetic parameters for the final model are listed in Table 2. Population means (95% CIs) of cellular kinetic parameters in a typical patient were T_{max} (T_{lag} + T_{gro}) 9.29 (8.81–9.70) days; doubling time (T_{dbl}) 0.755 (0.667–0.821) days; C_{max} 23,600 (18,900–29,900) copies/μg; initial decline half-life (HL_α) 5.00 (4.15–5.90) days; terminal half-life (HL_β) 352 (241–647) days; and fraction of C_{max} that appears in the β or terminal phase (F_β) 0.659 (0.529–0.820) percent. The final model included the following covariates: age on C_{max} and T_{dbl}; SPD per IRC before LDC on HL_α; tocilizumab and/or corticosteroid use (for the treatment of CRS and/or NEs) on C_{max}, HL_α, and T_{lag}; and LDH before LDC on T_{lag}. Covariate effects on model parameters are given as fold-change in Table 2. In patients aged 18 and 86 years, C_{max} was altered 2.49-fold and 0.24-fold, respectively, and T_{dbl} was altered 0.70-fold and 1.15-fold, respectively, relative to the median age of 63 years. In patients treated with tocilizumab and/or corticosteroids, C_{max} was 1.67-fold higher, HL_α was 2.31-fold longer, and T_{lag} was altered 0.62-fold, compared with patients who received neither tocilizumab nor corticosteroids. HL_α was altered 1.55-fold and 0.37-fold in patients with SPD per IRC of 419 cm^2 and 0.8 cm^2, respectively, relative to the median SPD per IRC of 22.5 cm^2. T_{lag} was altered 2.12-fold and 0.74-fold in patients with LDH of 11,900 U/L and 112 U/L, respectively, relative to the median LDH of 269 U/L.

Figure 2 shows the population-predicted and individual-predicted liso-cel transgene levels versus observed liso-cel

Table 1 Patients and clinical covariates of 261 patients with relapsed/refractory large B-cell lymphoma

Characteristic	All patients [$N = 261$]
Age at baseline, years [median (range)]	63 (18–86)
Body weight at baseline, kg [median (range)]	76.1 (40.1–182)
Body mass index at baseline, kg/m^2 [median (range)]	25.6 (16.8–51.6)
Creatinine clearance at baseline, mL/min[a] [median (range)]	92.2 (24.7–351)
Aspartate aminotransferase at baseline, U/L [median (range)]	22 (9–133)
Alanine aminotransferase at baseline, U/L [median (range)]	17 (3–157)
Lactate dehydrogenase before LDC, U/L [median (range)]	269 (112–11,900)
SPD (per IRC) before LDC, cm^2 [median (range)]	22.5 (0.8–419)
C-reactive protein at baseline, mg/L [median (range)]	27.3 (0.25–2160)
Total administered dose, 10^6 cells [median (range)]	91.1 (43.9–156)
Sex [*n* (%)]	
Male	168 (64)
Female	93 (36)
Race [*n* (%)]	
Caucasian	224 (86)
African American	12 (5)
Asian	11 (4)
Others	2 (1)
Multiple	1 (0.4)
Unknown	11 (4)
Ethnicity [*n* (%)]	
Hispanic/Latino	26 (10)
Non-Hispanic/Latino	226 (87)
Unknown	9 (3)
LVEF [*n* (%)]	
≥ 40% and < 50%	12 (5)
≥ 50%	249 (95)
Large B-cell lymphoma subtypes [*n* (%)]	
DLBCL NOS	135 (52)
DLBCL transformed from FL	59 (23)
DLBCL transformed from other iNHL subtypes	15 (6)
HGBCL	35 (13)
PMBCL	15 (6)
FL grade 3B	2 (1)
ECOG PS at screening [*n* (%)]	
0	107 (41)
1	150 (57)
2	4 (2)
Prior lines of systemic therapy [*n* (%)]	
1	8 (3)
2	120 (46)
3	67 (26)
≥ 4	66 (25)
Response to prior therapy [*n* (%)]	
Refractory	206 (79)
Relapsed	55 (21)
Chemotherapy response [*n* (%)]	
Refractory	174 (67)
Sensitive	87 (33)
Prior HSCT[b] [*n* (%)]	
Yes	92 (35)
No	169 (65)
Never achieved CR with prior therapy [*n* (%)]	
Yes	115 (44)
No	146 (56)

Table 1 (continued)

Characteristic	All patients [$N = 261$]
Secondary CNS lymphoma [*n* (%)]	
Yes	7 (3)
No	254 (97)
Bridging therapy [*n* (%)]	
Yes	154 (59)
No	107 (41)
Tocilizumab/corticosteroid use for CRS and/or NE treatment [*n* (%)]	
Either or both	73 (28)
Neither	188 (72)
Liso-cel single-dose level [*n* (%)]	
Dose level 1	44 (17)
Dose level 2	176 (67)
Dose level 3	41 (16)

CNS central nervous system, *CR* complete response, *CRS* cytokine release syndrome, *DLBCL* diffuse large B-cell lymphoma, *ECOG PS* Eastern Cooperative Oncology Group performance status, *FL* follicular lymphoma, *HGBCL* high-grade B-cell lymphoma with *MYC* and *BCL2* and/or *BCL6* rearrangements, *HSCT* hematopoietic stem cell transplantation, *iNHL* indolent non-Hodgkin lymphoma, *IRC* Independent Review Committee, *LDC* lymphodepleting chemotherapy, *LVEF* left ventricular ejection fraction, *NE* neurological event, *NOS* not otherwise specified, *PMBCL* primary mediastinal B-cell lymphoma, *SPD* sum of the product of perpendicular diameters

[a]Calculated using the Cockcroft–Gault equation

[b]Includes any prior autologous or allogeneic HSCT

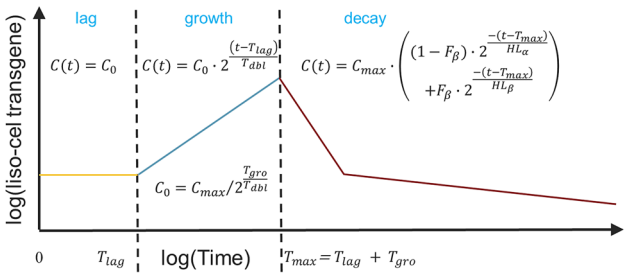

Fig. 1 Cellular kinetic model of liso-cel. C_0 initial transgene levels, C_{max} maximum transgene levels, F_β fraction of C_{max} that appears in the β or terminal phase, HL_α initial (α phase) decline half-life, HL_β terminal (β phase) half-life, T_{dbl} doubling time during growth phase, T_{gro} growth phase duration, T_{lag} lag phase duration, T_{max} time to maximum transgene levels

transgene levels for the final model. Data pairs (predicted, observed) that lie on the line of unity denote agreement between the model and observations. The model adequately captured the observations. Improvement in the population-predicted concurrence with the observed data is noted and expected due to the introduction of model covariates. Figure 2 also shows CWRES versus population-predicted and time after dose for the final model, which were acceptable and similar to results from the base model. Generally, no values fell outside |CWRES| > 5, indicating that no data points were classified as outliers. The residuals showed no trend by population-predicted or time, indicating no systemic biases in model fit in these dimensions. Figure 3 shows a visual predictive check between model-predicted and observed liso-cel transgene levels versus time after dose. The median and 5th/95th percentiles of the 500 replicate simulations were superimposed with the observation summaries. These simulations demonstrated that the model adequately captured the central tendency and variability in the observed data.

3.4 Simulations

Figure 4 shows the simulated $AUC_{0–28d}$, C_{max}, and T_{max} values from the final model, conditioned on the observed patient covariates in the data set and summarized over 300 replicate simulation studies. Median (5th–95th percentile) values across the simulations were 214,000 (26,100–1,560,000) day*copies/μg for $AUC_{0–28d}$, 27,300 (4260–146,000) copies/μg for C_{max}, and 9.00 (6.96–14.5) days for T_{max}. Covariates associated with C_{max} were also associated with $AUC_{0–28d}$. Both C_{max} and $AUC_{0–28d}$ increased with decreasing patient age. Both C_{max} and $AUC_{0–28d}$ tended to increase with increasing SPD per IRC before LDC. Furthermore, both C_{max} and $AUC_{0–28d}$ were higher and T_{max} was slightly shorter in patients receiving tocilizumab and/or corticosteroids. T_{max} tended to be longer with increasing LDH before LDC. The magnitude of effect on liso-cel expansion metrics demonstrated that the covariate associations were smaller than the residual BSV in the population.

Table 2 Population cellular kinetic parameter estimates of liso-cel and bootstrap evaluation

Parameter[a]	Interpretation	Estimate[b]	Estimate[b], %RSE	Estimate, 95% CI[c]	BSV	BSV, %RSE	BSV, 95% CI
T_{lag}, days	Lag phase duration	3.27	10.8	(2.71–3.97)	66.5	13.5	(49.7–79.6)
T_{gro}, days	Growth phase duration	6.02	5.6	(5.27–6.53)	–	–	–
C_{max}, copies/μg	Maximum liso-cel transgene levels	23,600	10.4	(18,900–29,900)	91.5	6.9	(78.4–105)
T_{dbl}, days	Doubling time during growth phase	0.755	5.3	(0.667–0.821)	21.0	13.6	(14.6–26.4)
F_{β}, fraction	Fraction of C_{max} that appears in the terminal (β) phase	0.00659	12.1	(0.00529–0.00820)	–	–	–
HL_{α}, days	Initial (α-phase) decline half-life	5.00	9.1	(4.15–5.90)	97.7	7.2	(83.9–114)
HL_{β}, days	Terminal (β-phase) half-life	352	23.0	(241–647)	–	–	–
RUV, %	Residual unexplained variability	91.5	3.0	(86.2–97.9)	–	–	–

Parameter[a]	Interpretation	Estimate[b]	Estimate[b], %RSE	Estimate, 95% CI[c]	As fold-change over covariate range
C_{max}~Age	Change in C_{max}, relative to age of 63 years	– 0.0330	14.4	(– 0.0401 to – 0.0201)	2.49, Age 18 years 0.24, Age 86 years
C_{max}~TocilCS	Change in C_{max} with Toci and/or CS use for CRS and/or NE treatment	0.670	43.1	(0.172–1.42)	1.67, TocilCS
HL_{α}~SPD	Change in HL_{α}, relative to SPD per IRC before LDC of 22.5 cm^2	0.187	19.0	(0.108–0.256)	0.37, SPD 0.8 cm^2 1.55, SPD 419 cm^2
HL_{α}~TocilCS	Change in HL_{α} with Toci and/or CS use for CRS and/or NE treatment	1.31	26.5	(0.744–2.25)	2.31, TocilCS
T_{dbl}~Age	Change in T_{dbl}, relative to age of 63 years	0.00660	27.3	(0.00308–0.00968)	0.70, Age 18 years 1.15, Age 86 years
T_{lag}~LDH	Change in T_{lag}, relative to LDH before LDC of 269 U/L	0.294	29.8	(0.137–0.499)	0.74, LDH 112 U/L 2.11, LDH 11,900 U/L
T_{lag}~TocilCS	Change in T_{lag} with Toci and/or CS use for CRS and/or NE treatment	– 0.384	18.5	(– 0.502 to – 0.199)	0.62, TocilCS

BSV between-subject variability, *CI* confidence interval, C_{max} maximum transgene levels, *CRS* cytokine release syndrome, *CS* corticosteroids, F_{β} fraction of C_{max} that appears in the β or terminal phase, HL_{α} initial (α phase) decline half-life, HL_{β} terminal (β phase) half-life, *IRC* Independent Review Committee, *LDH* lactate dehydrogenase, *NE* neurological event, *RSE* relative standard error, *RUV* residual unexplained variability, *SPD* sum of the product of perpendicular diameters, T_{dbl} doubling time during growth phase, T_{gro} growth phase duration, T_{lag} lag phase duration, *Toci* tocilizumab

[a]Parameter values were centered on the following values, reflecting the central tendency of the patient characteristics (age of 63 years, SPD of 22.5 cm^2, and LDH of 269 U/L) and no tocilizumab and/or corticosteroid use

[b]Estimate and estimate %RSE were given from the importance sampling step

[c]Estimate 95% CI was given from analysis of 500 replicate bootstrap fits, 4 of which failed with termination errors and were not included in these summaries

4 Discussion

Unlike systemic therapies, CAR T-cell therapies are administered once and the kinetics depend on CAR T-cell expansion, contraction, and persistence after infusion into the patient. Patient and disease characteristics are anticipated to play a role in the variability of cellular kinetics observed with CAR T-cell therapy. Liso-cel transgene observations were well described by a piecewise model of cellular growth kinetics that featured lag, exponential growth, and biphasic decay phases in treated patients. Unless otherwise specified, the following summaries are for a typical patient who was 63 years of age, had SPD before LDC (per IRC) of 22.5 cm^2, had LDH before LDC of 269 U/L, and did not use tocilizumab and/or corticosteroids for the treatment of CRS and/or NEs. Liso-cel transgene levels were stable during the lag phase (T_{lag}) and doubled approximately eight times during the growth phase (T_{gro}), reaching a C_{max} of 23,600 copies/μg (91.5% BSV) at 9.29 days ($T_{max} = T_{lag} + T_{gro}$). After peak levels, the liso-cel transgene decay phase was biphasic, with α-phase (HL_{α}) and β-phase (HL_{β}) half-life estimates of 5.00 (97.7% BSV) and 352 days, respectively. The fraction of peak liso-cel transgene levels appearing in the β-phase (F_{β}) was estimated at 0.659%. In this empirical cellular kinetic model, the fractions of α-phase and β-phase were assumed as effector and memory T cells, respectively.

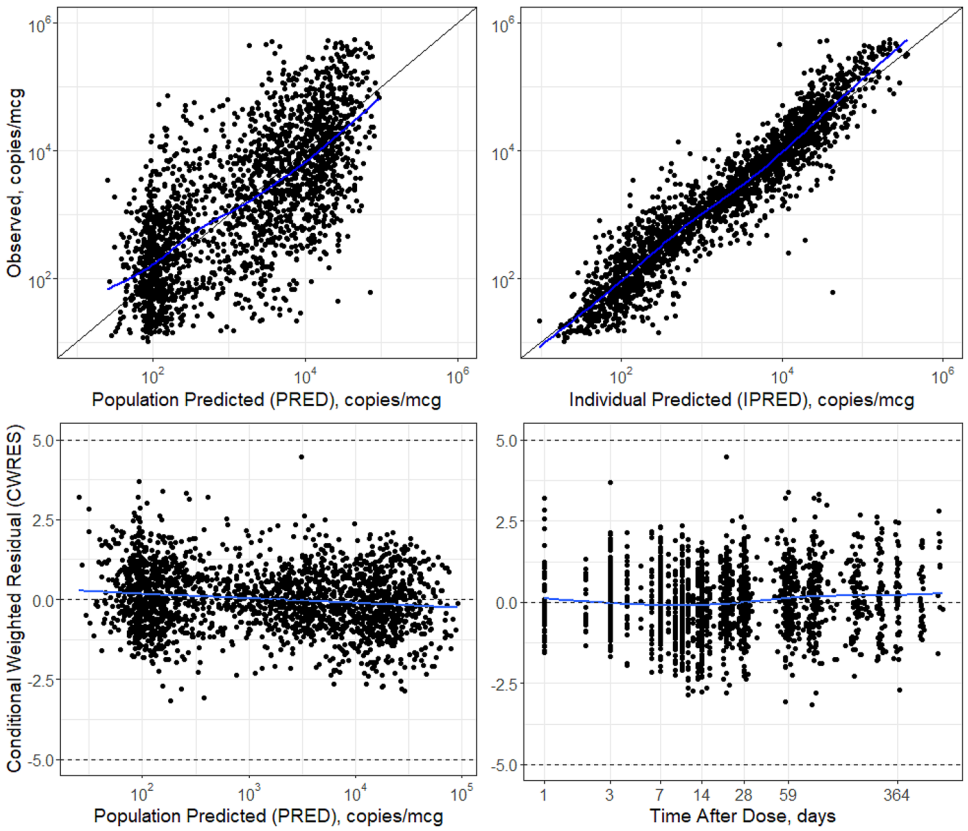

Fig. 2 Goodness-of-fit plots of the final population cellular kinetic model of liso-cel in patients with relapsed/refractory large B-cell lymphoma. For observed versus final model PRED and IPRED liso-cel transgene levels, a line of unity is superimposed as a black solid line. An LOESS smoothing function is superimposed as a blue solid line as a guide for the eye. For final model CWRES of liso-cel transgene levels over time and PRED liso-cel transgene levels, the expected central tendency of 0 and the outlier limits of −5 and +5 are superimposed as black, dashed horizontal lines. A LOESS smoothing function is superimposed as a blue solid line as a guide for the eye. *CWRES* conditional weighted residuals, *IPRED* individual-predicted, *LOESS* locally weighted smoothing line, *PRED* population-predicted

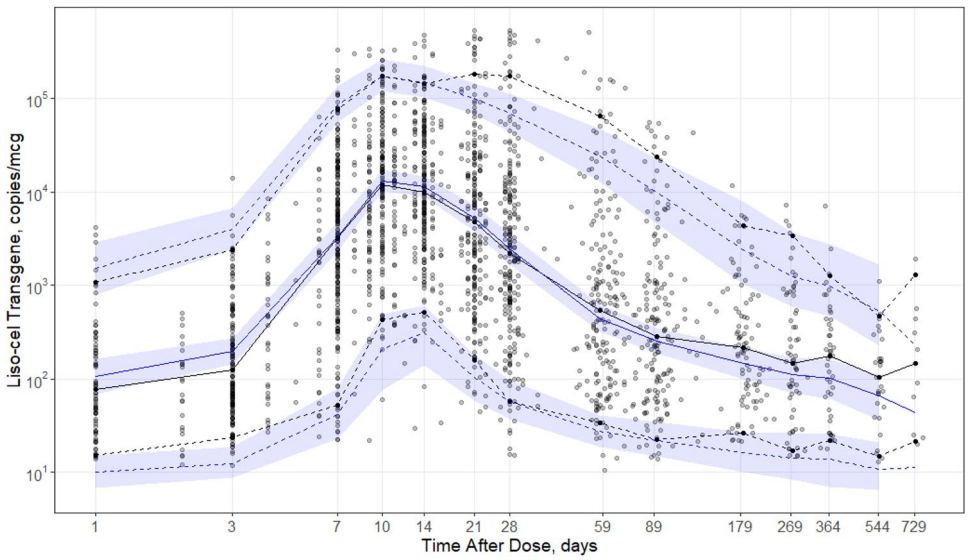

Fig. 3 Visual predictive check of the final population cellular kinetic model of liso-cel in patients with relapsed/refractory large B-cell lymphoma. Observed data (faint points) summarized by median (black solid line) and 5th/95th percentiles (black dashed lines), binned around nominal time points. Replicate model predictions are summarized at the same percentiles (blue solid line: median; blue dashed lines: 5th/95th percentiles) as the observed data and also provide 95% prediction intervals (blue shaded area) for the 500 replicate simulations. In the case of sparse data, prediction intervals were not generated. Log transformation was applied to both axes, emphasizing the first 4 weeks after a single infusion of liso-cel

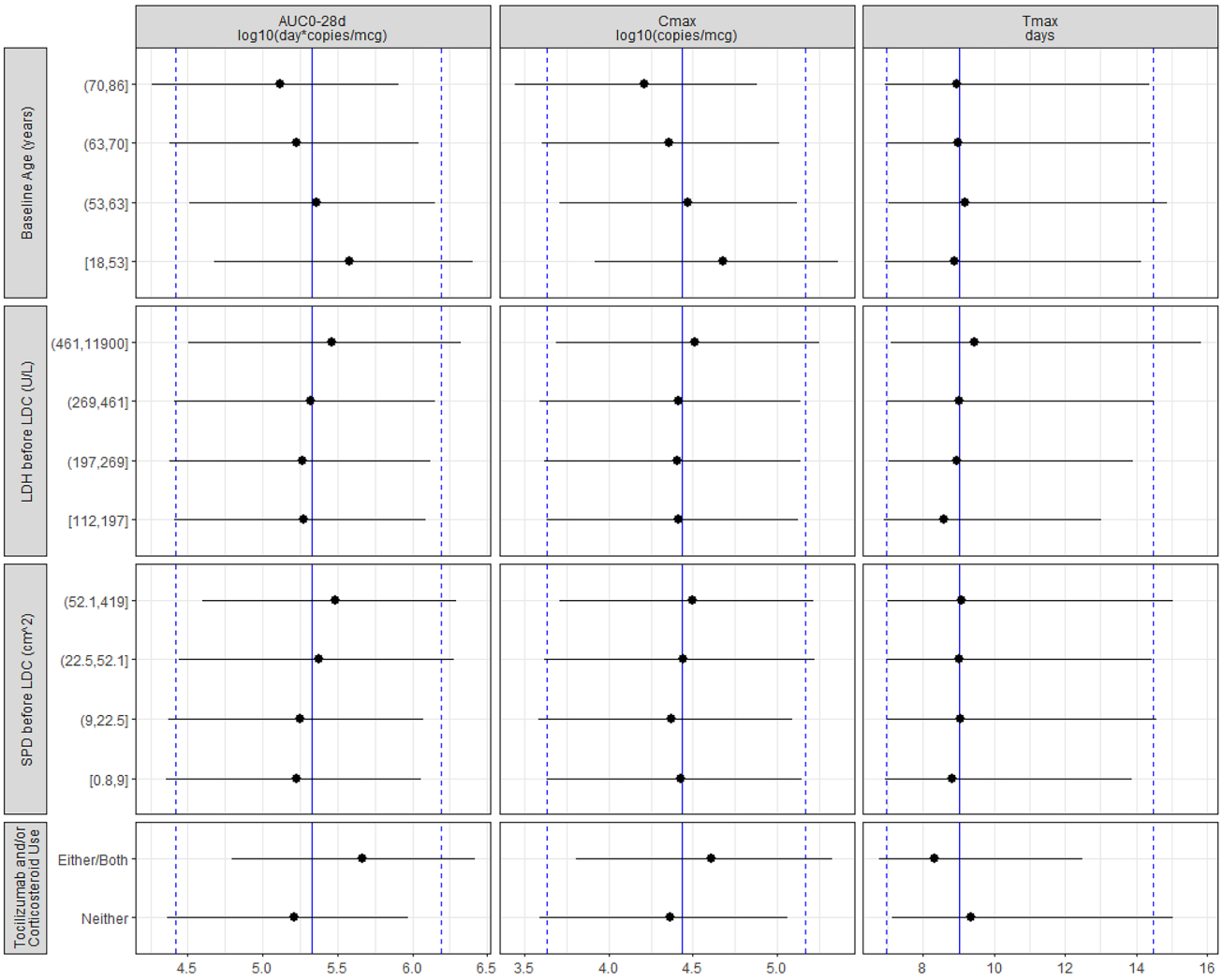

Fig. 4 Forest plot of model covariates on simulated $AUC_{0–28d}$, C_{max}, and T_{max}. Simulations were conditioned on the observed patient covariates ($n = 261$), and replicate ($m = 300$) simulations were conducted with between-subject variability. Blue vertical lines denote the overall simulation 50th (solid blue line) and 5th/95th (dashed blue lines) percentiles. Simulated expansion metrics were binned by covariate (quartiles of continuous covariates), and the 50th (black circle) and 5th/95th (black lines) percentiles are plotted for comparison. Tocilizumab and/or corticosteroid use refers to concomitant treatment with either/both agents or neither for the treatment of cytokine release syndrome or neurological events after liso-cel infusion. $AUC_{0–28d}$ area under the curve for transgene levels from 0 to 28 days post-infusion, C_{max} maximum transgene levels, *LDC* lymphodepleting chemotherapy, *LDH* lactate dehydrogenase, *SPD* sum of the product of perpendicular diameters, T_{max} time to maximum transgene levels

A covariate search using stepwise forward addition ($\alpha = 0.01$) and backward elimination ($\alpha = 0.001$) demonstrated that baseline age, SPD per IRC before LDC, LDH before LDC, and the use of tocilizumab and/or corticosteroids for the treatment of CRS and/or NEs were associated with liso-cel kinetics. Univariate effect sizes should be interpreted with caution as the covariates may be correlated. Therefore, the association of patient covariates was instead assessed by simulation of C_{max}, T_{max}, and $AUC_{0–28d}$ using the final model. Observed patient covariates were used to condition these simulations, thus preserving any collinearity in the covariates. Treatment with tocilizumab and/or corticosteroids was associated with higher C_{max} and $AUC_{0–28d}$. Higher C_{max} and $AUC_{0–28d}$ were also associated with CRS and/or NEs [1], which triggered the therapeutic intervention with tocilizumab and/or corticosteroids. In TRANSCEND, the median time to onset of CRS and NEs was 5.0 and 9.0 days, respectively [1], and the median time from onset of CRS to first administration of tocilizumab was 1.5 days [1]. Therefore, the relationship of tocilizumab/corticosteroid use with cellular kinetic parameters should be interpreted with caution. Examination of these cellular kinetic parameters across the covariate range (quartiles, in the case of continuous covariates) showed the expected

association pattern described in Fig. 4. The magnitude of effect on expansion metrics demonstrated that the covariate associations were smaller than the residual BSV in the population. Particularly, BSV not explained by covariates for C_{max} was estimated as 91.5%. Thus, the covariate effects were not considered meaningful.

Recent work with physiologically based pharmacokinetic models of exogenous T-cell administration found that the administered dose did not contribute to initial T-cell blood concentrations [22]. In this effort, a similar lack of dose dependence was noted with liso-cel transgene levels. Dose was examined as a covariate on model parameters but was not found to be statistically significant. This suggests that the dose was not associated with expansion quantities in the tested administered dose range ($44–156 \times 10^6$ CAR^+ T cells). Thus, no dose adjustment is recommended in specific populations [23]. Tisagenlecleucel also exhibited a flat relationship between dose and the cellular kinetic parameters ($0.2–5.0 \times 10^6$ CAR^+ T cells/kg in patients weighing ≤ 50 kg, and $0.1–2.5 \times 10^8$ CAR^+ T cells in patients weighing > 50 kg) [12].

Finally, these results can be compared with similar analyses conducted for tisagenlecleucel in pediatric and young adult patients with B-ALL [10] and axi-cel in adult patients with LBCL [19]. Prior literature reports for CAR T-cell therapies were based on a theoretic model developed by De Boer and Perelson [18] describing the murine immune response to an infection by *Listeria monocytogenes* or lymphocytic choriomeningitis virus. Findings from this present analysis are aligned with previous analyses conducted for other CAR T-cell therapies (expansion of CAR T cells post-infusion followed by biphasic decline). Two new concepts were introduced by this analysis: the introduction of the novel lag phase and the parameterization of the liso-cel transgene population cellular kinetic model. First, previous reports in the literature for CAR T-cell therapies did not report a lag phase after administration, but the general concept of a lag phase as living cells acclimatize to a new environment is well established [21, 24]. Parameterization of the population cellular kinetic model reported here differs from previous efforts, posing the model in more readily interpretable (but still interconvertible) terms. For example, exponents of base 2 were used (instead of base e), reflecting the underlying biology of mitotic doubling of cell populations. Furthermore, the doubling time of CAR T cells is expressed in this model instead of a fold-expansion from baseline ratioed to time to maximum liso-cel transgene levels. The model parameterizations are interconvertible with the previous formulation using the following relationships: $fold_x = C_{max}/C_0$; $\rho = \log(fold_x)/T_{gro}$; $\alpha = \log(2)/HL_\alpha$; $\beta = \log(2)/HL_\beta$ (definition of terms is available in the study by Stein et al. [10]). Doubling time, T_{max}, HL_α, and HL_β of tisagenlecleucel were 0.78, 9.3, 4.3, and 220 days, respectively [10], while doubling time, T_{max}, HL_α, and HL_β of axi-cel were 0.87, 4.9, 3.3, and 173 days, respectively [19]. Doubling time and HL_α of other CD19-directed CAR T-cell therapies were consistent with liso-cel kinetic parameters. T_{max} of axi-cel was earlier than that of tisagenlecleucel and liso-cel. HL_β of liso-cel was longer than that of tisagenlecleucel or axi-cel (352 vs. 220 or 173 days, respectively), which might be due to longer follow-up with liso-cel; however, the interpretation of these comparisons requires caution because of the limitations of the current analysis stated below.

This analysis was limited by the following factors. Random effects for T_{gro}, F_β, and HL_β were not estimated in the cellular kinetic model of liso-cel due to their high η shrinkage. T_{max} ($T_{lag} + T_{gro} = 9.29$ days) in this liso-cel model was slightly earlier than T_{max} reported by noncompartmental analysis (12 days) [1]. This discrepancy might be in part due to misspecification of the cellular kinetic model by no random effect of T_{gro}. Furthermore, HL_β had slightly high relative standard error (23.0%). Furthermore, the evaluation period (2 years for liso-cel and 1 year for tisagenlecleucel and axi-cel) was approximately two HL_β, which is relatively short for the robust estimation of HL_β. Therefore, the abovementioned comparison of HL_β among CD19-directed CAR T cells should be interpreted with caution. The following differences among CAR T-cell therapies should also be noted for the comparison of cellular kinetic parameters: defined composition (liso-cel) versus undefined composition (tisagenlecleucel and axi-cel); LBCL (liso-cel and axi-cel) versus B-ALL (tisagenlecleucel); and 4-1BB (liso-cel and tisagenlecleucel) versus CD28 (axi-cel) costimulatory domain. Earlier T_{max} of axi-cel compared with tisagenlecleucel and liso-cel might be explained in part by the finding that CD28 and 4-1BB co-stimulatory domains are associated with effector T-cell like phenotype and memory T-cell like phenotype, respectively [25]. No apparent relationship has been observed between the $CD8^+$:$CD4^+$ ratio and cellular kinetic parameters of tisagenlecleucel in LBCL and B-ALL [12, 13], suggesting that defined versus undefined composition might not be a crucial factor to determine cellular kinetics. The eligibility criteria in TRANSCEND is broad and aligns with recommendations for clinical trials of CAR T-cell therapies to maximize generalizability [26]; however, the findings cannot be extrapolated to the broader population (e.g. pediatric patients and patients with severe renal impairment). Nonetheless, the population cellular kinetic model of liso-cel adequately captured the central tendency and variability in observations from patients in TRANSCEND and indicated no systemic biases in model fit in the dimensions of time or predicted values.

5 Conclusion

Observed liso-cel transgene levels were well described by a piecewise model of cellular growth kinetics that featured lag, growth, and biphasic decay phases in treated patients. Covariates tested were not considered to have a meaningful impact on liso-cel kinetics.

Acknowledgements The authors are grateful for the support of their colleagues at Bristol Myers Squibb, with special thanks to Kathryn Newhall for guidance and support and Chang-pin Huang for data validation. All authors contributed to and approved the manuscript; writing and editorial assistance were provided by Amy Agbonbhase, Ph.D., of The Lockwood Group (Stamford, CT, USA), and was funded by Bristol Myers Squibb.

Declarations

Funding This study was funded by Juno Therapeutics, a Bristol-Myers Squibb Company.

Conflict of interest Ken Ogasawara, Timothy Mack, James Lymp, Justine Dell'Aringa, and Jeff Smith are employees of Bristol Myers Squibb and hold stock in Bristol Myers Squibb. Michael Dodds is a consultant for Bristol Myers Squibb.

Ethics approval The research was conducted within all the appropriate ethical and legal guidelines.

Consent to participate For investigations involving human patients, informed consent was obtained from the participants involved.

Consent for publication All authors approved this manuscript for submission.

Availability of data and material Bristol Myers Squibb policy on data sharing may be found at https://www.bms.com/researchers-and-partners/independent-research/data-sharing-request-process.html.

Author contributions KO and MD contributed to the study design and data analysis and interpretation. TM, JL, JD, and JS contributed to data acquisition and interpretation. KO drafted the manuscript. All authors critically reviewed the draft manuscript, approved the final version to be published, and agree to be accountable for all aspects of the work.

References

1. Abramson JS, Palomba ML, Gordon LI, Lunning MA, Wang M, Arnason J, et al. Lisocabtagene maraleucel for patients with relapsed or refractory large B-cell lymphomas (TRANSCEND NHL 001): a multicentre seamless design study. Lancet. 2020;396(10254):839–52.
2. Teoh J, Johnstone T, Christin B, Yost R, Haig N, Mallaney M, et al. Lisocabtagene maraleucel (liso-cel) manufacturing process control and robustness across CD19+ hematological malignancies [abstract]. Blood. 2019;134(Suppl 1):593.
3. Turtle CJ, Hanafi LA, Berger C, Hudecek M, Pender B, Robinson E, et al. Immunotherapy of non-Hodgkin's lymphoma with a defined ratio of CD8+ and CD4+ CD19-specific chimeric antigen receptor-modified T cells. Sci Transl Med. 2016;8(355):355ra116.
4. Paszkiewicz PJ, Fräßle SP, Srivastava S, Sommermeyer D, Hudecek M, Drexler I, et al. Targeted antibody-mediated depletion of murine CD19 CAR T cells permanently reverses B cell aplasia. J Clin Invest. 2016;126(11):4262–72.
5. Wang X, Chang WC, Wong CW, Colcher D, Sherman M, Ostberg JR, et al. A transgene-encoded cell surface polypeptide for selection, in vivo tracking, and ablation of engineered cells. Blood. 2011;118(5):1255–63.
6. Maus MV, Levine BL. Chimeric antigen receptor T-cell therapy for the community oncologist. Oncologist. 2016;21(5):608–17.
7. Kochenderfer JN, Somerville RPT, Lu T, Shi V, Bot A, Rossi J, et al. Lymphoma remissions caused by anti-CD19 chimeric antigen receptor T cells are associated with high serum interleukin-15 levels. J Clin Oncol. 2017;35(16):1803–13.
8. Neelapu SS, Locke FL, Bartlett NL, Lekakis LJ, Miklos DB, Jacobson CA, et al. Axicabtagene ciloleucel CAR T-cell therapy in refractory large B-cell lymphoma. N Engl J Med. 2017;377(26):2531–44.
9. Schuster SJ, Bishop MR, Tam CS, Waller EK, Borchmann P, McGuirk JP, et al. Tisagenlecleucel in adult relapsed or refractory diffuse large B-cell lymphoma. N Engl J Med. 2019;380(1):45–56.
10. Stein AM, Grupp SA, Levine JE, Laetsch TW, Pulsipher MA, Boyer MW, et al. Tisagenlecleucel model-based cellular kinetic analysis of chimeric antigen receptor-T cells. CPT Pharmacometrics Syst Pharmacol. 2019;8(5):285–95.
11. Mueller KT, Maude SL, Porter DL, Frey N, Wood P, Han X, et al. Cellular kinetics of CTL019 in relapsed/refractory B-cell acute lymphoblastic leukemia and chronic lymphocytic leukemia. Blood. 2017;130(21):2317–25.
12. Mueller KT, Waldron E, Grupp SA, Levine JE, Laetsch TW, Pulsipher MA, et al. Clinical pharmacology of tisagenlecleucel in B-cell acute lymphoblastic leukemia. Clin Cancer Res. 2018;24(24):6175–84.
13. Awasthi R, Pacaud L, Waldron E, Tam CS, Jäger U, Borchmann P, et al. Tisagenlecleucel cellular kinetics, dose, and immunogenicity in relation to clinical factors in relapsed/refractory DLBCL. Blood Adv. 2020;4(3):560–72.
14. YESCARTA (axicbatagene ciloleucel) [summary of product characteristics]. Amsterdam, The Netherlands: Kite Pharma EU B.V.; 2018.
15. KYMRIAH (tisagenlecleucel) [summary of product characteristics]. Dublin: Novartis Europharm Limited; 2018.
16. Lindbom L, Pihlgren P, Jonsson EN. PsN-Toolkit—a collection of computer intensive statistical methods for non-linear mixed effect modeling using NONMEM. Comput Methods Programs Biomed. 2005;79(3):241–57.

17. Bauer R. NONMEM Users Guide. Introduction to NONMEM 7.4.1. 2017. https://nonmem.iconplc.com/nonmem741. Accessed 30 Apr 2020.
18. De Boer RJ, Perelson AS. Quantifying T lymphocyte turnover. J Theor Biol. 2013;327:45–87.
19. US Food and Drug Administration. Pharmacometric review of axicabtagene ciloleucel. 2017. https://www.fda.gov/media/109140/download. Accessed 5 May 2020.
20. Savic RM, Karlsson MO. Importance of shrinkage in empirical Bayes estimates for diagnostics: problems and solutions. AAPS J. 2009;11(3):558–69.
21. Madigan M, Martinko J, Parker J. Brock biology of microorganisms. 8th ed. London: Prentice Hall, Inc.; 1997.
22. Khot A, Matsueda S, Thomas VA, Koya RC, Shah DK. Measurement and quantitative characterization of whole-body pharmacokinetics of exogenously administered T cells in mice. J Pharmacol Exp Ther. 2019;368(3):503–13.
23. BREYANZI (lisocabtagene maraleucel) [prescribing information]. Princeton, NJ: Bristol Myers Squibb; 2021.
24. Zwietering MH, Jongenburger I, Rombouts FM, van 't Riet K. Modeling of the bacterial growth curve. Appl Environ Microbiol. 1990;56(6):1875–81.
25. Salter AI, Ivey RG, Kennedy JJ, Voillet V, Rajan A, Alderman EJ, et al. Phosphoproteomic analysis of chimeric antigen receptor signaling reveals kinetic and quantitative differences that affect cell function. Sci Signal. 2018;11(544):eaat6753.
26. Jaggers JL, Giri S, Klepin HD, Wildes TM, Olin RL, Artz A, et al. Characterizing inclusion and exclusion criteria in clinical trials for chimeric antigen receptor (CAR) T-cell therapy among adults with hematologic malignancies. J Geriatr Oncol. 2021;12(2):235–8.